

Synthesis of Zeolite A from Iraqi Natural Kaolin Using a Conventional Hydrothermal Synthesis Technique

Ali Mohammed Salih^{1*}, Craig Williams², Polla A Khanaqa¹

¹Department of Geology, Kurdistan Institution for Strategic Studies and Scientific Research, Sulaimani, Kurdistan Region- F. R. Iraq

²Department of Chemistry and Forensic Science, School of Biology, Faculty of Science and Engineering, University of Wolverhampton, UK

*Corresponding author's email: shwangeology@yahoo.com

Received: 12-01-2020

Accepted: 15-07-2020

Available online: 31-12-2020

ABSTRACT

The synthesis of zeolite materials by hydrothermal transformation of kaolin using a conventional hydrothermal method was investigated. Different analytical techniques were used to characterize the starting kaolin and produced zeolite A samples, including scanning electron microscopy (SEM), energy-dispersive spectroscopy (EDS), x-ray diffraction (XRD), x-ray fluorescence (XRF), thermogravimetric analysis (TGA), and Fourier transform infrared (FT-IR) spectroscopy. The synthetic zeolite type A was obtained after activation of kaolin and metakaolin followed by different thermal and chemical treatments. The metakaolinization phase was achieved by calcining the kaolin in air at 600°C for 3 hours, a much lower temperature than previously reported in the literature. Metakaolin was treated with 3 M sodium hydroxide solution at a ratio of 1:5 and, using stainless steel autoclaves with teflon liners, heated the mixture to 200°C in a microwave for 24 hours. The results from this synthesis route showed that zeolite A with a cubic crystal habit has been successfully synthesized.

Keywords: Zeolite A, Kaolin, Metakaolin, Hydrothermal synthesis

1. INTRODUCTION

Zeolites are well-known aluminosilicate that have been used widely as adsorbents in separation and purification processes and in the control of environmental pollution. Zeolites are used in various industrial applications owing to their high cation-exchange ability and molecular sieve and catalytic properties (Dyer and Zubair 1998; Ramos et al., 2004). Both natural zeolites and synthetic zeolites have important uses such as in petrochemical cracking, wastewater treatment, nuclear energy generation, as a

landfill liner, in contaminated land remediation, and, more recently, in several emerging fields of health and medicine (Alvarez-Ayuso et al., 2003; Ackley et al., 2003). Furthermore, in comparison with the natural zeolites, synthetic zeolites have shown greater efficiency in the treatment of wastewater owing to their excellent adsorption capacities and high performances.

Previous studies have revealed that the preparation of synthetic zeolites from chemical sources of silica and alumina are more expensive when compared with the conversion of raw materials (i.e., natural sources of silica and alumina) into zeolitic materials using hydrothermal transformation (Querol et al., 1997; Tanaka et al., 2004; Adamczyk and Bialecka 2005; Walek et al., 2008; Kovo and Holmes 2010). Trials continued to improve the

such as type A, mordenite, and X, Y, P zeolites, which are derived from cheaper raw materials, such as clay

Access this article online

DOI: 10.25079/ukhjs.v4n2y2020.pp11-23

E-ISSN: 2520-7792

Copyright © 2020 Salih et al. Open Access journal with Creative Commons Attribution Non-Commercial No Derivatives License 4.0 (CC BY-NC-ND 4.0)

minerals, coal ashes, natural zeolites, municipal solid wastes, and industrial sludge (Inglezakis et al., 2004; Pandey et al., 2009; Novembre et al., 2011).

Among these naturally available raw materials, kaolin, which has a silica to alumina ratio of nearly 1, similar to zeolite A, has been used as an alternative cheap raw material for the synthesis of zeolite A (Miao et al., 2009). Currently, synthetic zeolites are used more often in the commercial setting than natural zeolites owing to the homogeneity of their particle sizes and the purity of the crystalline products (Szoztak, 1998).

Kaolin ($\text{Al}_2\text{O}_3 \cdot 2\text{SiO}_2 \cdot 2\text{H}_2\text{O}$) is a rock or sedimentary deposit rich in kaolinite and other very similar clay minerals, such as dickite, nacrite, and halloysite. Kaolin is also known as “China clay.” It was discovered in the year 1867 and the word “kaolin” is derived from the name of the Chinese town Kao-Ling located in the Jiangxi Province of southeast China (Paul, 2003; Pohl, 2011). The basic kaolin mineral structure comprises layers of a single tetrahedral silica (SiO_4) sheet and a single octahedral alumina [$\text{Al}(\text{O}, \text{OH})_6$] sheet joined by sharing a common layer of oxygen and hydroxyl units (Deer et al., 1992). The low reactivity of kaolin is demonstrated in the difficulties that are encountered when it used in a chemical synthesis method (Murat et al., 1992), and accordingly, kaolin first needs to be decomposed by calcination at temperatures of between 550°C and 950°C to obtain the metakaolin phase formed following the loss of structural water and the subsequent reorganization of the structure (Lambert et al., 1989). Kaolin undergoes a series of phase transformations when thermally treated. The formation of metakaolin during thermal treatment is an essential step, which depends on the following 3 reactions (Scheme 1): destruction of the kaolin sheet structure, dehydroxylation and the recombination of silica and alumina to form the structure of metakaolin (Rios et al., 2007).

During the past decades, numerous studies have focused on minimizing the synthesis cost of good quality, pure zeolite A with a high crystallinity. Many studies have focused on the optimization of the main factors known to strongly effect the type and degree of crystallinity of the synthesized zeolite A, including the method of preparation, the type of mineralizer, concentration, and

time (Rios et al., 2007; Ugal et al., 2010; Mousa and Buhl, 2014).

The concentration of the base is one of the most important parameters that control the crystallization of zeolites. The increase in alkalinity causes an increase in the crystallization rate via both nucleation and crystal growth (Wang et al., 2008).

In this study, local natural kaolin from Iraq was used as the starting material to produce zeolite A using a hydrothermal synthesis technique, enabling the exploitation of the large clay mineral deposits available, which is abandoned mainly as kaolin.

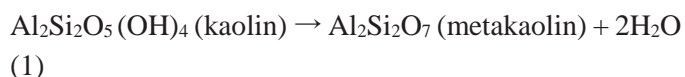
2. EXPERIMENTAL WORK

2.1. Synthetic zeolite procedure

The kaolin samples were crushed and milled into powder using a porcelain mortar before being sieved using laboratory soil sieves. The mesh sizes selected for the collection of the kaolin particles were $75 \mu\text{m} < dp < 125 \mu\text{m}$. Synthesis of zeolite A from kaolin involved the following 2 basic steps: the first step involved metakaolinization, which is the thermal treatment of the raw kaolin at a high temperature of 600°C for 3 hours, and the second step was the chemical treatment of the prepared metakaolin with 3 M sodium hydroxide (NaOH).

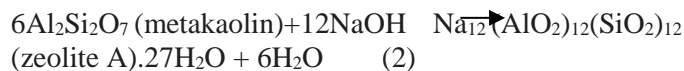
2.2. Calcination (metakaolinization) and synthesis of zeolite A

The conventional hydrothermal synthesis technique was used in which 50 grams of kaolin clay powder (with particle sizes of $<125 \mu\text{m}$) was calcined at 600°C for 3 hours to convert the kaolin to metakaolin (Scheme 2). This caused a change in the structure of the kaolin, which was accompanied by the evolution of volatile matter leading to the formation of the metakaolin, as shown in the following equation:



The produced metakaolin was subsequently treated with 3 M NaOH solution in a ratio of 1:5 and, using stainless

steel autoclaves with a teflon liner, heated the mixture to 200°C for 24 hours in order to insert the sodium ions into the metakaolin structure, as shown by the following reaction:



The treated kaolin clay was then washed 3 times with deionized water to remove the excess unreacted NaOH. It was subsequently filtered and dried in an oven at 100°C overnight as shown in Scheme 2. Various samples with different NaOH concentrations were prepared in order to study the optimum concentration required for the synthesis of zeolite A.

2.3. Characterization of the untreated and thermally treated kaolin

The physical and chemical characteristics of the samples were studied using the following analytical techniques:

2.3.1. Scanning electron microscopy

The surface morphology of the kaolin and zeolite A samples was determined using a ZEISS EVO50 scanning electron microscope (SEM) under the following analytical conditions: electron high tension (EHT) = 10.00 kV and 20.00 kV; signal A = secondary electron (SE) 1 and variable pressure secondary electron (VPSE); WD = 6.0, 6.5, 7.0, and 8.5 mm at different magnifications. The SEM micrographs in Figures 1 and 2 show the appearances of the kaolin products obtained before and after hydrothermal treatment of kaolin and metakaolin.

2.3.2. Energy-dispersive spectroscopy

The energy-dispersive spectroscopy (EDS) (Oxford INCA) analytical technique was used in this study for the analysis of the elemental composition or chemical characterization of the Iraqi kaolin and zeolite A samples. The main elements and their corresponding oxides were determined by EDS. The localizations of the 4 analyzed sites were designated by numbers and a typical EDS spectrum.

2.3.3. X-ray diffraction

X-ray diffraction (XRD) is an analytical technique used for the phase identification of natural kaolin and zeolite A materials and in this study, an Empyrean PANalytical x-ray diffractometer with copper K-alpha radiation at 40 mA and 40 kV and secondary monochromation was used. All of the data collection was obtained in the $2^\circ \theta$ range at a starting position of 5° and an end position of 50° or 80° , with a scanning step of $0.02^\circ \theta$. The results of the crystalline patterns were compared with the standard line pattern database supplied by the International Centre for Diffraction Data.

2.3.4. X-ray fluorescence spectroscopy

The analysis of the elemental composition of the raw Iraqi kaolin and the prepared zeolite was obtained using an LXE, PANalytical x-ray fluorescence (XRF) spectrometer with a 50 kV energy x-ray tube. The chemical analysis of the Iraqi kaolin in the “as received” form was studied.

2.3.5. Thermogravimetric analysis

The thermal stabilities of the raw Iraqi kaolin and the Iraqi metakaolin were obtained using thermogravimetric analysis (TGA) on a Perkin Elmer TGA7 thermobalance between 30°C and 1000°C. A heating rate of 20°C/min was applied under a nitrogen atmosphere. Thermal analysis methods were used to obtain information about the mass loss change and adsorption or crystallization. The transition of Iraqi kaolin to Iraqi metakaolin was observed at about 570°C.

2.3.6. Fourier transform infrared spectroscopy

An ALPHA (Brucker) Fourier transform infrared (FT-IR) spectrometer with a single platinum attenuated total reflectance (ATR) diamond module was used for the analysis of the materials in this study. The FT-IR spectra of the raw materials were recorded in the range of 400 to 4000 cm^{-1} . The FT-IR spectra of the original and thermally treated kaolin were investigated at 600°C, 950°C, and 1000°C.

3. RESULTS AND DISCUSSION

The micrographs of the “as received” Iraqi kaolin samples are presented in Figure 1. The images were obtained using SEM analysis under the following SEM analytical

conditions: EHT = 10.00 kV, Signal A = SE1, and WD 6.0 mm at a magnification of 20000 \times . The micrograph in Figure 1 shows that the crystals of the Iraqi kaolin is not well defined and that the crystallites are in a random orientation before any modification. Kaolin can be recognized by its platy morphology, which is composed of small, loosely packed hexagonal plates (Mousa and Buhl, 2014). In contrast, the micrographs of the Iraqi metakaolin samples were obtained using the following SEM analytical conditions: EHT = 10.00 kV, Signal A = SE1, and WD = 6.5 mm at a magnification of 20000 \times and 10000 \times . The samples were calcined at 600 $^{\circ}$ C for 3 hours. The micrographs show the randomly oriented crystallites and, in particular, indicate the appearance of the hexagonal plates (Figure 2). The micrographs of the synthesized zeolite A samples were obtained under the following SEM analytical conditions: EHT = 10.00 kV, Signal A = SE1, and WD = 7 mm at magnifications of 5000 \times and 10000 \times . As shown in Figures 3 and 4, the micrographs indicate, in particular, the well-formed, typical cubic-shaped crystals of zeolite A with an average particle size of 3.1 μ m.

The main chemical composition of the kaolin and the existence of SiO₂ and Al₂O₃ in the raw kaolin as an aluminosilicate source used in this study are presented in Table 1. The results of the EDS and XRF analysis show that the predominant exchangeable cations in the kaolin structure are Na⁺, K⁺, Mg²⁺, and Ca²⁺ (Figure 5). The results of the chemical analysis of zeolite type A obtained after the conversion of the raw materials into zeolitic materials are also presented in Table 1. The predominant exchangeable cations for zeolite A was found to be Na⁺, K⁺, Mg²⁺, and Ca²⁺. The results indicate that the major zeolite components in the structure are SiO₂, Al₂O₃, Na₂O, and K₂O, in addition to trace amounts of impurities associated with the raw kaolin that was used in the preparation, which could not be removed under the studied conditions. The predominant exchangeable cations for zeolite A were found to be Na⁺, K⁺, Mg²⁺, and Ca²⁺, which verify the results of the EDS analysis and concur with the results obtained by Ugal et al., (2010). It is worth mentioning that the treatment of kaolin under the strong basic conditions generated by NaOH results in an increase in the sodium content from 1.64% to 14.624% and leads to a decrease in the silicon content from 50.72% to 35.95%, as well as in the aluminum content from 31.49% to 27.47% in the corresponding zeolite samples (Doaa and Mohamed, 2014).

The raw kaolin contained quartz as a major impurity. Kaolin can be identified by its characteristic XRD peaks at 12.23 $^{\circ}$ and at 24.82 $^{\circ}$ 2 θ (Zhao et al., 2004; Gougazeh and Buhl, 2010). However, kaolin contains minor impurities of illite, muscovite, and halloysite. A variety of XRD patterns for the kaolin transformation phases at different temperatures are presented in Figure 6, including the untreated, "as received" kaolin and the thermally treated kaolin materials at 600 $^{\circ}$ C, 950 $^{\circ}$ C, and 1000 $^{\circ}$ C. The XRD patterns for the treated kaolin show a significant difference in comparison with the untreated kaolin sample, which was characterized by the disappearance of the diffraction peaks of kaolin and the appearance of amorphous aluminosilicate patterns (Mousa and Buhl, 2014). Metakaolin is an amorphous material and the highest diffraction peaks correspond to the presence of quartz (SiO₂), which is the crystalline phase in metakaolin (Mousa and Buhl, 2014). The XRD pattern for zeolite type A, as prepared by the conventional hydrothermal synthesis method, is shown in Figure 7.

The XRD plot for the synthesized zeolite A, with both the "a" and "b" marked lines indicating a database match, indicates the presence of 2 difference phases. The "a" lines indicate the presence of zeolite A (73%), while the "b" lines represent the presence of sodalite (27%), as determined by phase quantification according to the Rietveld method. The effect of the NaOH concentration (2, 4, 5, and 6 M NaOH) is shown in Figure 8. Analyzing the XRD data of the prepared samples showed the appearance of the characteristic peaks of zeolite A occurring at 3 M NaOH; however, zeolite A did not form at 2, 4, 5, and 6 M NaOH. The optimum crystallinity is obtained with 3 M NaOH, concurring with similar data obtained by Ayele et al. (2015), who synthesized zeolite material from activated kaolin samples that were reacted with 3 M NaOH. Furthermore, Mousa and Buhl (2014) found that a concentration of 1.5 to 3.5 M of NaOH is ideal for the synthesis of zeolite A. In this study, a concentration of 3 M of NaOH was found to be ideal for the synthesis of zeolite A.

Information about the weight loss change and structural transformations of kaolin was obtained using DTA/TGA techniques at a temperature range of between 30 $^{\circ}$ C and 1000 $^{\circ}$ C (Figure 9). As expected, dehydration occurred during the first stage at temperatures below 400 $^{\circ}$ C during which the weakest part of the chemical bond was broken or disturbed. Subsequently, dehydroxylation occurred in

the temperature range of 450°C and 600°C. During this stage of the transformation, the kaolin is transformed to the metakaolin phase with the loss of structural hydroxyl groups. At a temperature range of between 925°C and 950°C, a progressive decomposition occurs in which metakaolin converts to spinel. The DTG curve of the kaolin sample (Figure 9) shows a prominent peak at 570°C owing to dehydroxylation and at 980°C owing to the formation of a new solid phase. The total loss calculated from the thermogravimetric analysis was 23.5%.

Kaolin can be transformed into metakaolin at temperatures above 570°C. The dehydration of kaolin begins at between 550°C and 600°C during which disordered metakaolin is produced, with the continuous loss of hydroxyl ions up to a temperature of 900°C (Rios et al., 2007; Gougazeh and Buhl, 2010). According to Kakali, et al. (2001), kaolin dehydroxylation occurs at temperatures between 400°C and 650°C, which is the stage of transformation to metakaolin (Kakali et al., 2001). Frost et al. (2003) determined that this kaolin dehydroxylation process occurs between 450°C and 550°C. However, in this study, the dehydroxylation process occurred between 450°C and 600°C.

During calcination of kaolin, the silicon atoms experience a range of reactions with different distortion owing to dehydroxylation (Bellotto, 1995). The aluminum atoms mostly transform from an octahedral to a tetrahedral geometry. As the calcination temperature increases, the structure becomes more distorted and amorphous silica is then formed (Bellotto, 1995). The dehydroxylation process might cause a disturbance of the $\text{Al}(\text{O},\text{OH})_6$ octahedral sheet at the outer hydroxyls, but it does not have much effect on the SiO_4 tetrahedral sheets owing to the more stable inner hydroxyl groups (Rios et al., 2007). The outer hydroxyls of the octahedral sheets may be removed more easily by heating than the inner hydroxyls, which will maintain a more ordered SiO_4 tetrahedral group in the structure during dehydroxylation (Rios et al., 2007). After heating at 950°C, the SiO_4 groups combine with the AlO_6 group to form the Al-Si spinel phase, which has a short-range ordered structure (Bellotto, 1995).

The results from the TGA/DTG analysis show that the zeolite A sample underwent continuous weight loss during the stepwise heating to 900°C owing to

dehydration and dehydroxylation (Figure 10). According to Perraki and Orfanoudaki (2004), weight loss below 200°C is caused by losses of hygroscopic and loosely bonded water.

FT-IR spectra of the raw materials were recorded in the range of 400 to 4000 cm^{-1} . FT-IR spectra of the untreated and thermally treated kaolin were investigated at 600°C, 950°C, and 1000°C. Figure 11 shows the FT-IR spectra of the “as received” kaolin before calcination. The peaks at 3692 and 3620 cm^{-1} can be attributed to the stretching vibration of the hydroxyl groups in the kaolin structure (Saikia et al., 2003; Perraki and Orfanoudaki, 2004; Zhao et al., 2004).

The peaks at 3620 cm^{-1} were attributed to the stretching vibration modes of the inner hydroxyl groups, which are the OH groups located in the octahedral and tetrahedral sheets. The peaks at 3692 cm^{-1} correspond to the stretching vibration modes of the inner surface OH groups, which are positioned at the surface of the octahedral sheets of the adjacent kaolin layer (Kristof, 1993).

The 1115 cm^{-1} peak can be attributed to the stretching vibration of the Si-O bonds in the kaolin structure (Figure 11), whereas the peaks at 1034 cm^{-1} and 1002 cm^{-1} are caused by lattice vibrations of both the Si-O-Si and Si-O-Al bonds (Van der Marel and Beutelspacher, 1976). Frost et al. (2002) assigned the bending vibrations of the OH groups to the peaks at 910 cm^{-1} and 942 cm^{-1} corresponding to the “surface OH bends” and the “inner OH bends.” According to Van der Marel and Beutelspacher (1976), these bending vibrations of the OH groups are mainly caused by the bonds in the Al-OH groups (Sinha et al., 1995). The peaks at 795 cm^{-1} and 749 cm^{-1} were assigned to the Si-O-Si bonds and finally, the 456 cm^{-1} and 522 cm^{-1} peaks were assigned to deformation of the vibration of the Si-O bonds.

Figure 12 shows the transformation process of kaolin to metakaolin. The conversion of kaolin to metakaolin is revealed by the disappearance of these characteristic peaks. The peaks of metakaolin, located at 796 cm^{-1} and 801 cm^{-1} , which are assigned to the Si-O-Al bonds, can be observed (Lambert et al., 1989). The vibration band at 1076 cm^{-1} for metakaolin was assigned to the stretching of the Si-O-Si bonds, as reported in the previous studies (Sinha et al., 1995; Valcke et al., 1997; Qiu et al., 2004).

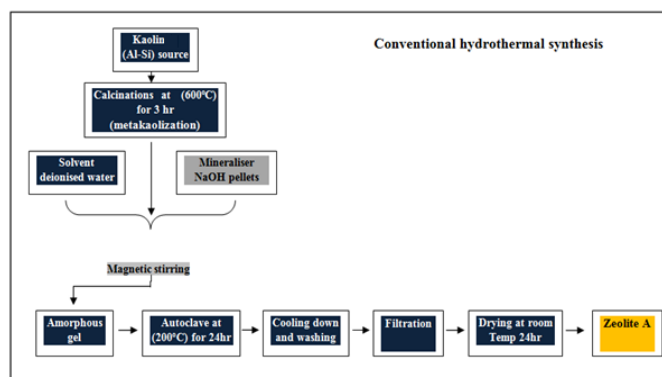
Table 1. The chemical composition (% wt.) of the kaolin and zeolite type A using EDS and XRF analytical techniques

Element		Na ₂ O%	MgO%	Al ₂ O ₃ %	SiO ₂ %	K ₂ O%	CaO%	TiO ₂ %	Fe ₂ O ₃ %
Kaolin	EDS	1.64	0.23	13.49	15.72	0.22	0.76	0.70	1.04
	XRF	1.74	0.21	30.17	39.37	0.48	0.89	0.78	1.49
Zeolite A	EDS	4.624	0.104	17.47	25.95	0.159	0.79	0.56	1.16
	XRF	4.744	0.114	16.47	23.95	0.179	0.69	0.66	1.26

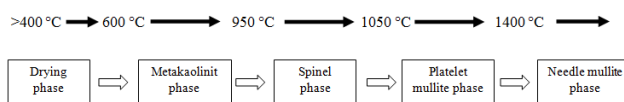
The presence of these bands confirmed the conversion of kaolin to the metakaolin phase, which was obtained from the calcined kaolin.

The 1034 cm⁻¹ peak of metakaolin was shifted to 960 cm⁻¹ (Fig. 12), which could be assigned to the antisymmetric stretching of the Si-O-Si or Si-O-Al bonds in the aluminosilicates with a zeolite structure (Nesse, 2000). A peak of weak intensity was observed around 549 cm⁻¹, indicating the presence of zeolite A in the cubic prism form (Figure 13). It could represent the beginning of the crystallization of a zeolite with double rings (Alkan

et al., 2005). The peaks at 456 cm⁻¹ correspond to the internal linkage vibrations of the Si-O-Si or Si-O-Al tetrahedral structures and to the asymmetric stretching of zeolite A. The transformation of kaolin to zeolite A can be observed clearly in the FT-IR spectra in the lattice region 960 to 456 cm⁻¹ (Fig. 13). The kaolin starting material gives well-defined FT-IR spectra bands in this region owing to the Si-O, Si-O-Al, and Al-OH vibrations.



Scheme 1. Flow diagram to indicate the various steps in the process of transforming Iraqi kaolin to zeolite type A by thermal treatment



Scheme 2. A flowchart showing the conversion of the raw materials into zeolitic materials conducted by conventional hydrothermal synthesis

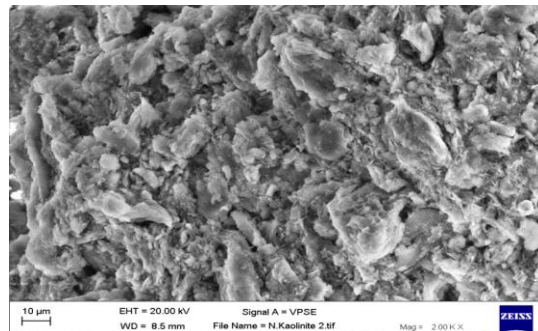


Figure 1. SEM micrograph of kaolin showing the crystalline nature of kaolin at a magnification of 2000x

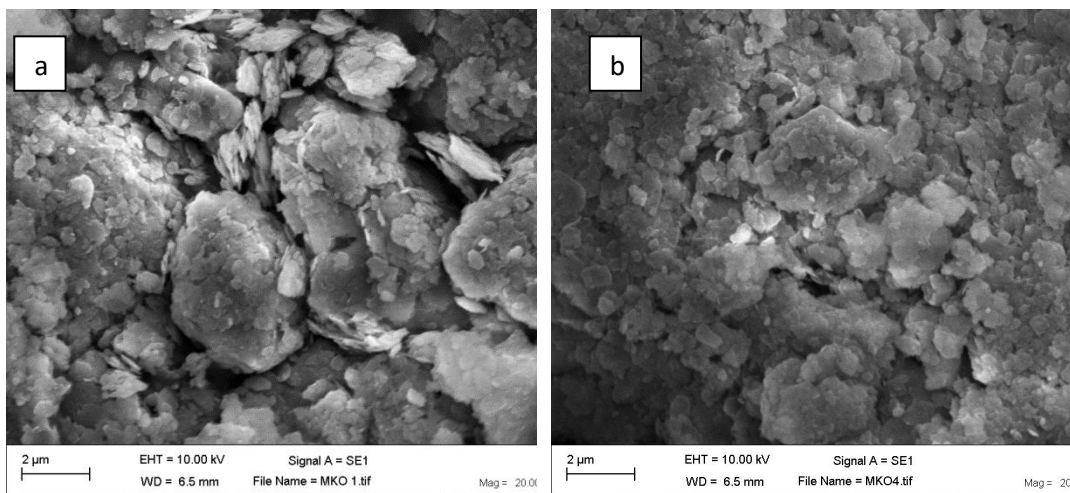


Figure 2. SEM micrographs showing the crystalline nature of metakaolin at a magnification of (a) 20000x and (b)10000x

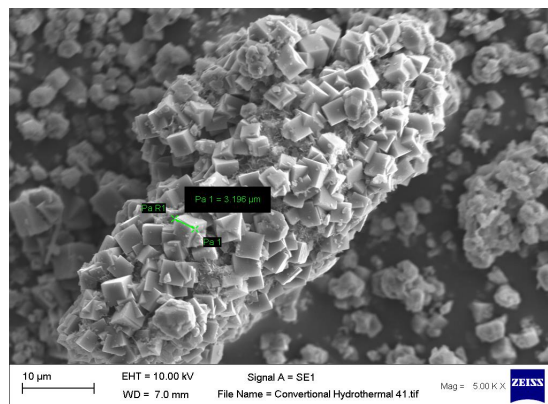


Figure 3. A SEM micrograph showing the orientation of the crystallites obtained using a conventional hydrothermal synthesis reaction at a magnification of 5000x

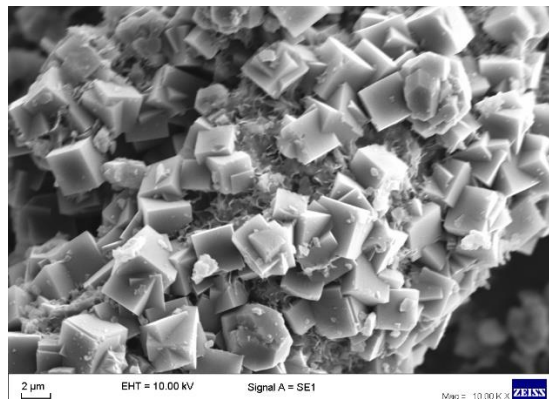


Figure 4. A SEM micrograph showing the orientation of the crystallites obtained using a conventional hydrothermal synthesis reaction at a magnification of 10000x

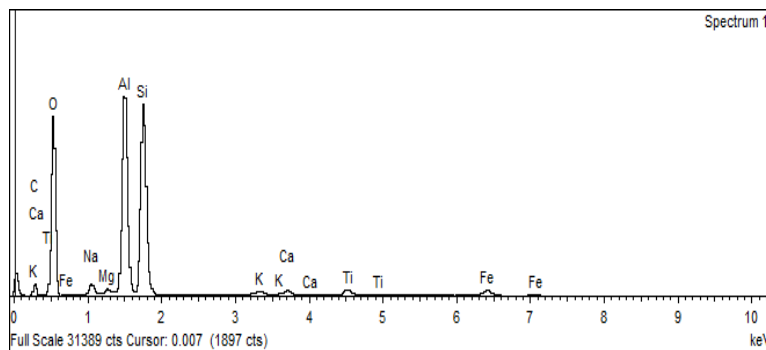


Figure 5. Spectral analysis showing the elemental composition of the kaolin sample

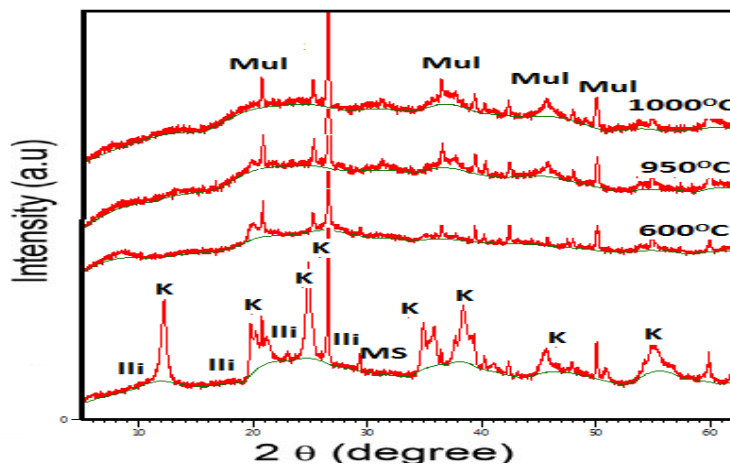


Figure 6. XRD patterns of the untreated and calcined kaolin at different temperatures. Illi, illite; K, kaolin; Ms, muscovite; Mul, mullite

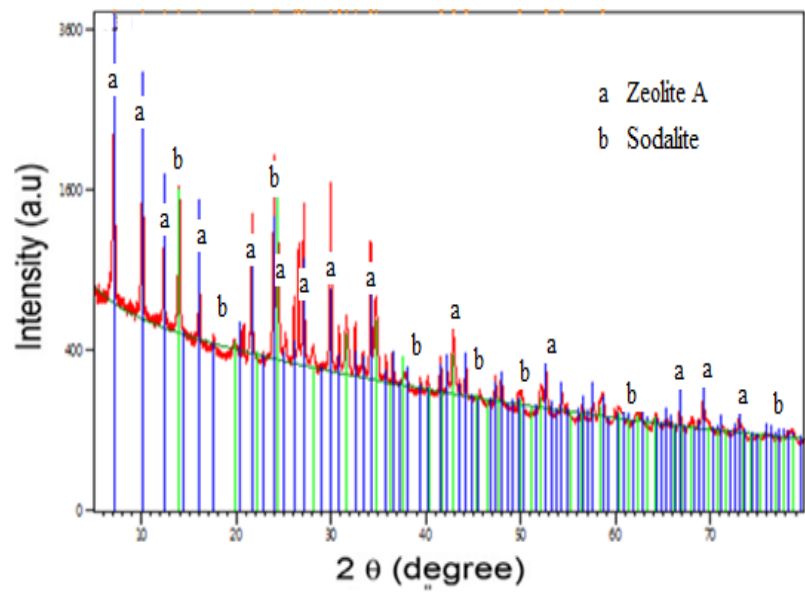


Figure 7. XRD Graphic analysis showing the mineralogical XRD analysis of zeolite A and sodalite

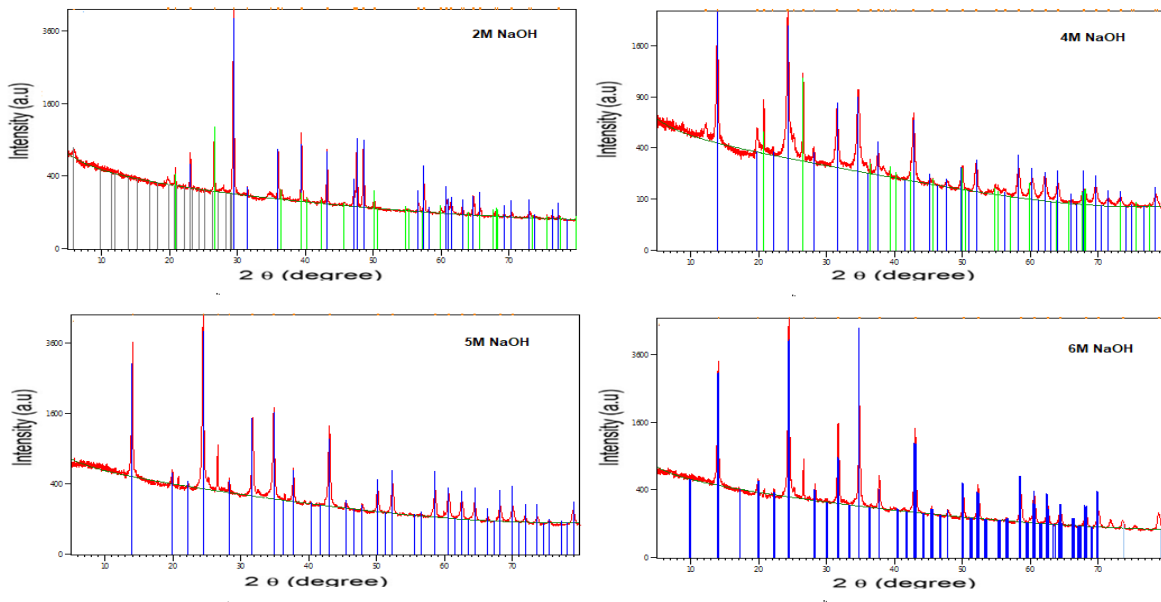


Figure 8. XRD graphic analysis showing the mineralogical XRD analysis on the the effect of various NaOH concentrations (2, 4, 5, and 6 M NaOH)

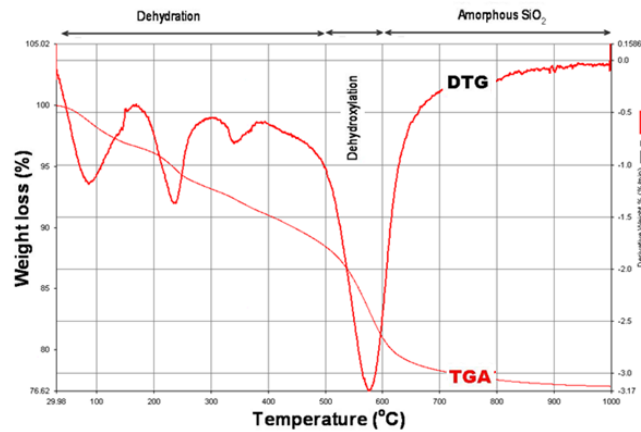


Figure 9. Thermogravimetric analysis (TGA/DTG) of Iraqi kaolin showing the events between 30°C and 1000°C

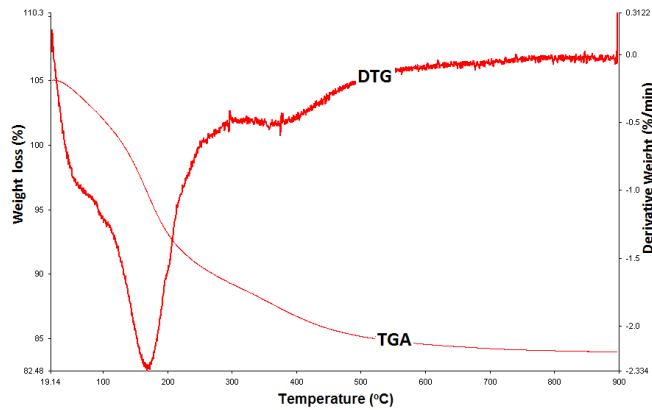


Figure 10. The thermogravimetric analysis (TGA/DTG) of zeolite A prepared by conventional hydrothermal synthesis routes showing the curves between 20°C and 900°C

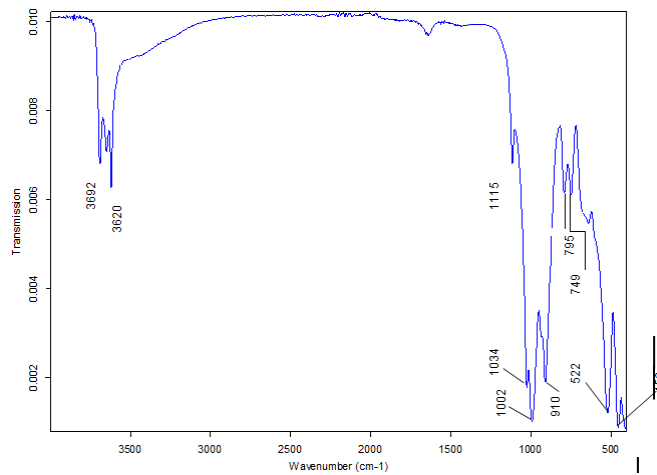


Figure 11. The FT-IR spectra obtained for the “as received” kaolin before calcinations

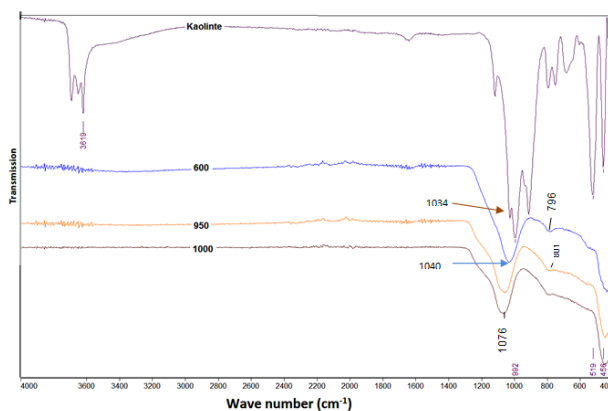


Figure 12. The FT-IR spectra of kaolin and metakaolin obtained after calcination of kaolin at 600°C, 950°C, and 1000°C

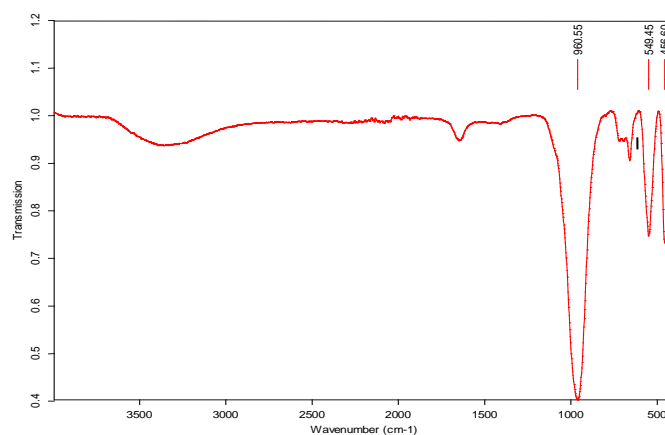


Figure 13. The FT-IR spectra of zeolite A obtained from kaolin after treatment

4. CONCLUSIONS

Following evaluation of the results obtained, the following conclusions can be drawn:

- Iraqi kaolin proved to be suitable for the production of zeolite type A following heating at 600°C for 3 hours, paving the way for the provision of local, low cost adsorbents that can be used in the removal of pollutants from wastewater and the reduction of material waste products.
- Applying both the EDS and XRF techniques revealed that SiO₂, Al₂O₃, Na₂O, and K₂O are the main components of kaolin and zeolite A. The analysis also showed that the predominant exchangeable cations in the kaolin and zeolite A structures are Na⁺, Mg²⁺, K⁺, and Ca²⁺, which remained unchanged during the dehydration and dehydroxylation transformations of kaolin.
- Optimization of the synthesis parameters for zeolite A from Iraqi kaolin was achieved for the first time. The parameters that were optimized are as follows: a base of 3 M NaOH, a crystallization time of 24 hours, a temperature of 200°C, and a 24-hour time interval for gel-formation conditions. By following these parameters, synthesis of zeolite A with a high crystallinity of about 90% in the cubic crystal form was achieved.
- The findings from the FT-IR spectra as well as the DTA/TGA measurements showed that the metakaolin phase can be obtained by heating the kaolin at 600°C for 3 hours.

- Finally, from the physicochemical characterization results, it can be concluded that the Iraqi kaolin used in this study has properties suitable for zeolite synthesis and could be, in principle, a useful source of silica and alumina.

REFERENCES

- Ackley M.W., Rege S.U. and Saxena H. (2003) Application of natural zeolites in the purification and separation of gases. *Microporous and Mesoporous Materials*, 61 (1–3), 25 – 42.
- Adamczyk, Z. and Bialecka, B. (2005) Hydrothermal synthesis of zeolites from polish coal fly ash. *Polish Journal of Environmental Studies*, 14(6), 713 – 719.
- Alkan, M., Hopa, C., Yilmaz, Z. and Guler, H. (2005) The effect of alkali concentration and solid/liquid ratio on the hydrothermal synthesis of zeolite NaA from natural kaolin. *Microporous and Mesoporous Materials*, 86, 176 – 184.
- Alvarez-Ayuso, E., Garcia-Sanchez, A. and Querol, X. (2003) Purification of metal electroplating waste waters using zeolites. *Water Research*, 37(20), 4855 – 4862.
- Ayele, L., Perez-Pariente, J., Chebude, Y. and Diaz, I. (2015) Synthesis of zeolite A from Ethiopian kaolin. *Microporous and Mesoporous Materials*, 215, 29 – 36.
- Bellotto, M., Gualtieri, A., Artioli, G., and Clark, S.M. (1995) Kinetic study of the kaolinite-mullite reaction sequence. Part I: kaolinite dehydroxylation. *Physics and Chemistry of Minerals*, 22 (4), 207–214.
- Deer, W.A., Howie, R.A., and Zussman, J. (1992) An introduction to the rock-forming minerals. 2nd ed. Harlow: Longman.
- Doaa, M. and Mohamed, S. (2014) Removal of Pb²⁺ from water by using Na-Y zeolites prepared from Egyptian kaolins collected from different sources. *Journal of Environmental Chemical Engineering*, 2, 723 – 730.
- Dyer, A. and Zubair, M. (1998) Ion-exchange in Chabazite. *Microporous and Mesoporous Materials*. 22, 135 – 150.
- Frost, R.L., Horváth, E., Makó, E., Kristóf, J. and Rédey, A. (2003) Slow transformation of mechanically dehydroxylated kaolinite to kaolinite - an aged mechanochemically activated formamide - intercalated kaolinite study. *Thermochimica Acta*, 408, 103 – 113.
- Frost, R.L., Mako, E., Krsitof, J. and Klopogge, J.T. (2002). Modification of kaolin surfaces through mechanochemical treatment - a mid-IR and near-IR spectroscopic study, *Spectrochimica Acta Part A. Molecular and Biomolecular Spectroscopy*, 58, 2849 – 2859.
- Gougazeh, M. and Buhl, C.H. (2010) Geochemical and Mineralogical Characterisation of the Jabal Al-Harad Kaolin Deposit, Southern Jordan for its Possible Utilization Clay Miner. *Mineralogical Society*, 45 (4), 281–294.
- Inglezakis, V.J., Loizidou, M.M. and Grigoropoulou, H.P. (2004) Ion exchange studies on natural and modified zeolites and the concept of exchange site accessibility. *Journal of Colloid and Interface Science*, 275(2), 570 – 576.
- Kakali, G., Perraki, T., Tsvilis, S., and Badogiannis, E. (2001). Thermal treatment of kaolin: the effect of mineralogy on the pozzolanic activity. *Applied Clay Science*, 20, 73 – 80.
- Kovo, A.S. and Holmes S.M. (2010) Effect of aging on the synthesis of kaolin-based zeolite Y from Ahoko Nageria using a novel metakaolnization technique. *Journal of dispersion Science Technology*, 31, 442 – 448.
- Kristof, J., Mink, J., Horvath, E. and Gabor, M. (1993). Intercalation study of clay minerals by Fourier transform infrared spectrometry. *Vibrational Spectroscop.*, 5, 61 – 67.
- Lambert, J.F., Minman, W.S. and Fripiat, J.J. (1989). Revisiting kaolin dehydroxylation: A silicon-29 and aluminum-27 MAS NMR study. *Journal of the American Chemical Society*, 111, 3517– 3522.
- Liu, Q., Spears, D.A. and Liu, Q. (2001). MAS NMR study of surface-modified calcined kaolin. *Applied Clay Science* 19, 89 – 94.
- Miao, Q., Zhou, Z., Yang, J., Lu, J., Yan, S. and Wang, J. (2009) Synthesis of NaA zeolite from kaolin source. *Frontiers of Chemical Engineering in China*, 3(1) 8 – 11.
- Mousa, G. and Buhl, J. (2014) Synthesis and Characterisation of zeolite A by hydrothermal transformation of natural Jordanian kaolin. *Journal of the Association of Arab Universities for Basic and Applied Sciences* 15, 35 – 42.
- Murat, M., Amorkrane, A., Bastide, J.P. and Montanaro, L. (1992) Synthesis of zeolites from thermally activated kaolinite. Some observations on nucleation and growth. *Clay Minerals*, 27, 119 – 130.
- Nesse W.D. (2000) Introduction of mineralogy, Oxford University Press.
- Novembre, D., Sabatino, B.D. and Gimeno, D. (2011) Synthesis and Characterisation of Na-X, Na-A and Na-P zeolites and hydroxysodalite from metakaolinite Clays. *Clay Minerals*, 46, 339 –354.
- Pandey, P., Sami, S.S., Sharma, S.K. and Singh, S. (2009) Batch Adsorption Studies for the Removal of Cu (II) Ions by ZeoliteNaX from Aqueous Stream. *Proceedings of the World Congress on Engineering and Computer Science*, I, San Francisco, USA.
- Paul W.S. (2003). "Kaolin". *New Georgia Encyclopedia*. <http://www.georgiaencyclopedia.org/nge/Article.jsp?id=h-1178>. Retrieved 2008-08-01.
- Perraki, T. and Orfanoudaki, A. (2004) Mineralogical study of zeolites from Pentalofofos area. *Applied Clay Science*, 25, 9.
- Pohl, Walter L. (2011). *Economic geology: principles and practice: metals, minerals, coal and hydrocarbons. Introduction to formation and sustainable exploitation of mineral deposits*. Chichester, West Sussex: Wiley-Blackwell. p. 331. ISBN 978-1-4443-3662-7.
- Qiu, G., Jiang, T., Li, G., Fan, X. and Huang, Z. (2004) Activation and removal of silicon in kaolin by thermochemical process. *Journal of Metallurg.*, 33, 1211 – 28.
- Querol, X., Plana, F., Alastuey, A., Lopez-Soler A. (1997) Synthesis of Na-zeolites from fly ash. *Fuel*, 76, 793 – 799.
- Ramos R.L., Armenta G.A., Gutierrez L.V.G., Coronado R.M.G., and Barron J.M. (2004) Ammonia exchange on clinoptilolite from mineral deposits located in Mexico. *Journal of Chemical Technology and Biotechnology*, 79, 651 – 657.
- Rios, C.A., Williams, C.D. and Maple M.J. (2007) Synthesis of zeolites and zeotypes by hydrothermal transportation of kaolin and metakaolin, *BISTUA*, 5 (1), 15–26.
- Saikia, N.J., Bharali, D.J., Sengupta, P., Bordoloi, D., Goswamee, R.L., Saikia, P.C. and Bothakur, P.C. (2003) Characterisation, beneficiation and utilization of a kaolin clay from Assam, India. *Applied Clay Science*, 24, 93 –103.
- Sinha, P.K., Paniker, P.K. and Amalraj, R.V. (1995) Treatment of radioactive liquid waste containing caesium by indigenously

- available synthetic zeolites: A comparative study. *Waste Management*, 15, 149 – 157.
- Szoztak, R. (1998) *Molecular Sieves: Principles of Synthesis and Identification*. 2nd ed. Blackie Academic and Professional: London.
- Tanaka, H., Miyagawa, A., Eguchi, B., Hino V.R. (2004) Synthesis of a pure-form Zeolite A from coal fly ash by dialysis. *Journal of Industrial and Engineering Chemistry*, 43, 6090 – 6094.
- Ugal, J.R, Hassan,K.H. and Inam H. Ali(2010) Preparation of type 4A zeolite from Iraqi kaolin: Characterisation and properties measurements, *Journal of the Association of Arab Universities for Basic and Applied Sciences*, 9, 2 – 5
- Valcke, E., Engels, B. and Cremers, A. (1997) The use of zeolites as amendments in radiocaesium- and radiostrontium-contaminated soils: A soil-chemical approach. Part II: Sr-Ca exchange in clinoptilolite, mordenite and zeolite A. *Zeolites*, 18, 212 – 217.
- Van der Marel, H.W. and Beutelspacher, H. (1976) *Atlas of Infrared Spectroscopy of Clay Minerals and Their Admixtures*, 1st ed. Elsevier: Amsterdam.
- Walek, T.T., Saito, F. and Zhang, Q. (2008) the effect of low solid/liquid ratio on hydrothermal synthesis of zeolites from fly ash. *Fuel*, 87, 3194 – 3199
- Wang, C.F., Li, J.S., Wang, L.J., Sun, X.Y. (2008) Influence of NaOH concentrations on synthesis of pure-form zeolite A from fly ash using two-stage method, *Journal of Hazardous Materials*, 155, 58 – 64.
- Zhao, H., Deng, Y., Harsh, J.B., Flury, M. and Boyle, J.S. (2004) Alteration of kaolin to cancrinite and sodalite by simulated hanford tank waste and its impact on cesium retention. *Clays and Clay Minerals*, 52, 1 – 13.